Microring-resonator-based add-drop filters in SiN: fabrication and analysis

Tymon Barwicz, Miloš A. Popović, Peter T. Rakich, Michael R. Watts, Hermann A. Haus, Erich P. Ippen, and Henry I. Smith

Research Laboratory of Electronics, Massachusetts Institute of Technology
77 Massachusetts Ave, Cambridge, MA 02139 USA
tymon@mit.edu

Abstract: Third-order add-drop filters based on series-coupled microring resonators were fabricated in silicon-rich silicon nitride with accurate dimensional control and negligible sidewall roughness. For the first time, a low 3 dB drop loss is demonstrated with a wide 24 nm free-spectral-range in a high-order microring filter without using the Vernier effect. The spectral response is matched by rigorous numerical simulation, and non-idealities in the drop- and through-port responses are shown to be of design origin and to be correctable.

OCIS codes: (130.0130) Integrated Optics; (230.5750) Resonators; (230.4000) Microstructure Fabrication; (060.4230) Multiplexing

References and links

1. B.E. Little, S.T. Chu, H.A. Haus, J.S. Foresi and J.-P. Laine, "Microring resonator channel dropping filters," J. Lightwave Technol. **15**, 998-1005 (1997).
2. B.E. Little, "Advances in microring resonators," presented at the Integrated Photonics Research Conference, Washington, DC, USA, 16-20 Jun. 2003.
3. Y. Yanagase, S. Suzuki, Y. Kokubun and S.T. Chu, "Box-like filter response and expansion of FSR by a vertically triple coupled microring resonator filter," J. Lightwave Technol. **20**, 1525-1529 (2002).
4. J.V. Hryniewicz, P.P. Absil, B.E. Little, R.A. Wilson and P.-T. Ho, "Higher order filter response in coupled microring resonators," IEEE Photon. Technol. Lett. **12**, 320-322 (2000).
5. B.E. Little, "A VLSI Photonic Platform," in *Proceedings of Optical Fiber Communication Conference*, (Optical Society of America, Washington, DC, 2003), vol. 2, pp. 444-445.
6. M. R. Watts, "Wavelength switching and routing through evanescently induced absorption," MS Thesis, Dept. of Electrical Eng. and Computer Sc., Massachusetts Institute of Technology, Cambridge MA, 2001.
7. T. Barwicz and H.I Smith, "Evolution of line-edge-roughness during fabrication of high index-contrast microphotonic devices," J. Vac. Sci. Technol. B **21**, 2892-2896 (2003).
8. C. Manolatou, M.A. Popovic, P.T. Rakich, T. Barwicz, H.A. Haus and E.P. Ippen, "Spectral anomalies due to coupling-induced frequency shifts in dielectric coupled resonator filters," presented at the Optical Fiber Communication Conference, Los Angeles, CA, USA, 22-27 Feb. 2004.
9. R. Grover, V. Van, T. A. Ibrahim, P. P. Absil, L. C. Calhoun, F. G. Johnson, J. V. Hryniewicz, and P.-T. Ho, "Parallel-cascaded semiconductor microring resonators for high-order and wide-FSR filters," J. Lightwave Technol. **20**, 900-905 (2002).
10. B.E. Little, S.T. Chu, J.V. Hryniewicz and P.P. Absil, "Filter synthesis for periodically coupled microring resonators," Opt. Lett. **25**, 344-346 (2000).

1. Introduction

Microring resonators allow for compact channel add-drop filters [1]. They have an important application in optical add-drop multiplexers (OADMs), key components for modern optical networks. Add-drop filters in OADMs must show low loss, flat passbands, and a wide free-spectral-range (FSR) that covers a significant part of the C-band. Recently, sixth-order microring resonator filters have been demonstrated in moderate index-contrast (~17%) with

#4002 - $15.00 US Received 9 March 2004; revised 26 March 2004; accepted 29 March 2004

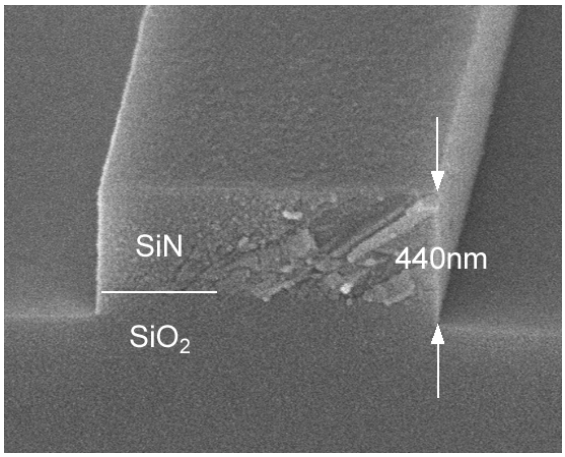

Fig. 1. Cross-section of a waveguide. See Table 1 for waveguide parameters.

low drop loss (<2dB) and flat passbands [2]. However, these filters suffer from a narrow FSR of about 6.4 nm, which is inadequate for OADMs where an FSR of about 30 nm is desired. For some applications, Vernier operation (rings of different radii) can be used to suppress non-synchronous ring resonances and extend the FSR as in [3]. However, this technique introduces intolerable dispersion into through channels at the suppressed resonances. Thus, it cannot be used for add-drop filters in OADMs where the through-port response is of critical importance. To increase the FSR, a higher index contrast (>100%) must be used to reduce the ring radius while keeping bending loss within acceptable bounds. Unfortunately, high index contrast (HIC) invites a number of difficulties in design and fabrication, and previous attempts at demonstrating high-order filters have met limited success [4].

In this paper, we report on third-order series-coupled microring add-drop filters fabricated in silicon-rich silicon nitride (SiN). For the first time, low drop loss (3dB) and a wide FSR (24 nm) are demonstrated in high-order HIC filters without using the Vernier effect. The drop loss is improved by 10 dB over previously reported wide-FSR filters [4]. The FSR is improved by more than a factor of 2 over moderate-index-contrast filters with only a 2 dB penalty in the drop-loss [5]. Further, the spectral response of the filter is matched to excellent agreement by rigorous numerical simulations. The latter show that the remaining filter shortcomings are not due to the material system or fabrication limitations, but are rather of design origin and are correctable. Thus, we defend HIC as a promising approach to add-drop filters.

Table 1. Waveguide Parameters

Parameter	Designed	Measured
SiN thickness	330 nm	314 nm
SiN index of refraction	2.200 at λ=1.55 μm	2.217 at λ=1.55 um
SiO_2 thickness	2.50 μm	2.53 μm
SiO_2 index of refraction	1.445 at λ=1.55 μm	1.455 at λ=1.55 μm
Etch depth	430 nm	440 nm

Most waveguides were 1050-nm-wide. Some bus waveguides were 850- or 650-nm-wide for enhanced coupling to the rings. Layer thicknesses and indices of refraction were measured with a Sopra spectroscopic ellipsometer, while the etch depth was measured with a Dektak profilometer.

#4002 - $15.00 US Received 9 March 2004; revised 26 March 2004; accepted 29 March 2004

2. Design

Our objective was to design add/drop filters with a 40 GHz passband and a 24 nm FSR in the C-band. Sensitivity of resonance frequencies and bus-ring and ring-ring coupling to dimensional variations makes polarization-independent operation difficult to achieve in HIC. Therefore, we designed filters to operate in only the TE polarization (electric field in the plane of the substrate). We rely on a polarization-diversity scheme to obtain polarization-independent operation. It involves splitting the polarizations and rotating one to obtain identical on-chip polarizations [6].

A waveguide cross-section is shown in Fig. 1. A single core layer of SiN on a SiO_2 cladding was used for bus waveguides and rings, with air top and side cladding. Designed and measured waveguide parameters are presented in Table 1. The rings were designed to support a high-Q (about 30 000) fundamental TE mode, but to suppress TM and higher-order TE resonant modes within the desired spectral range. Rings were chosen instead of racetrack resonators [4] as they have a higher uncoupled radiation Q for a given resonator path length. Using known synthesis techniques [1], the third-order filters were designed with a flat-top (Chebyshev) drop-port response. A simplified coupled-mode theory (CMT), based on that in the appendix of [1] but in 3D, was used to convert desired power couplings to bus-ring and ring-ring coupler spacings.

3. Fabrication

Fabrication of HIC microring resonators requires high-resolution lithography, strict dimensional control, and smooth sidewalls. Consequently, our fabrication process was based on direct-write scanning-electron-beam lithography (SEBL) and non chemically-amplified resist. In addition, the process was optimized to reduce sidewall roughness using the scheme described in [7].

Silicon wafers were first thermally oxidized to form the SiO_2 cladding. Then, the SiN core was deposited by low-pressure chemical-vapor-deposition (LPCVD) in a vertical thermal reactor using a gas mixture of SiH_2Cl_2 and NH_3. This deposition method yields a SiN with low stress and low hydrogen-content. Hence, the material exhibits low birefringence and negligible absorption in the telecommunication bands. The vertical thermal reactor provides excellent on wafer uniformity and a repeatable wafer-to-wafer distribution of film thicknesses and indices of refraction. The discrepancy between the designed and the employed SiN thickness (Table 1) is due to a problem with the optical characterization tool used in the clean room to select the device wafer. Next, 200 nm of poly-methyl-methacrylate (PMMA) and 40 nm of Aquasave were spun on. PMMA is a positive e-beam resist while Aquasave is a water-soluble conductive polymer from Mitsubishi Rayon used to prevent charging during SEBL. The PMMA was exposed at 30 KeV using a Raith 150 SEBL system. The Aquasave was removed, and the PMMA developed. Next, 50 nm of Ni was evaporated on the structure, and a liftoff performed by removing the non-exposed PMMA. Using the Ni as a hardmask, the waveguides were defined by conventional reactive-ion-etching (RIE). Vertical and smooth sidewalls where obtained with a gas mixture of CHF_3-O_2 in a 16:3 flow-ratio. To obtain an accurate etch depth, the RIE was performed in several steps, between which the etch depth was measured with a profilometer. Finally, the Ni was removed using a nitric-acid-based commercial wet Ni etchant. A third-order microring filter is presented in Fig. 2.

This process yielded high resolution, accurate dimensional control, and smooth sidewalls. Ring-to-bus gaps as small as 50 nm were successfully fabricated with good repeatability. Strict dimensional control was confirmed by feature size measurements using the Raith 150 in scanning-electron-microscope (SEM) mode. Accurate measurements were obtained by calibrating the deflection of the electron beam to the movement of the interferometric stage. During fabrication, the e-beam dose was selected to generate a correct bus waveguide width at the coupling region. This width was found to be accurate within the error of the measurement (about 5 nm). However, as proximity effect corrections were not applied, repeatable waveguide-width errors reaching 20 nm were observed on parts of the structure.

#4002 - $15.00 US Received 9 March 2004; revised 26 March 2004; accepted 29 March 2004

4. Optical characterization

Transmission measurements were performed using a modulated tunable laser coupled to the input facet of each waveguide from an optical fiber using a high-numerical-aperture-lens assembly. The output signal was detected with a large-area Ge photodetector through a non-dispersive microscope objective and filtered using a lock-in amplifier.

As input-to-drop loss is extracted by comparing the drop and through responses, these two measurements were performed under similar conditions and repeated several times with two different collection methods. A measurement of the response of a third-order microring filter is shown in Fig. 3. The filter shows 3 dB drop loss, a 24 nm FSR, a 1dB-bandwidth of 88 GHz and 7.5 dB of in-band rejection.

Fabry-Perot loss measurements, performed on several straight waveguides, are consistent with an upper bound for propagation loss of 3.6 dB/cm. Numerical simulations indicate that the loss is mainly due to e-beam field-stitching errors. A rotational error in the field calibration created a 30 nm offset of the bus waveguides every 100 μm, resulting in a loss of 0.021 dB/junction or 2.1 dB/cm. Thus, loss due to sidewall roughness and material absorption is below 1.5 dB/cm.

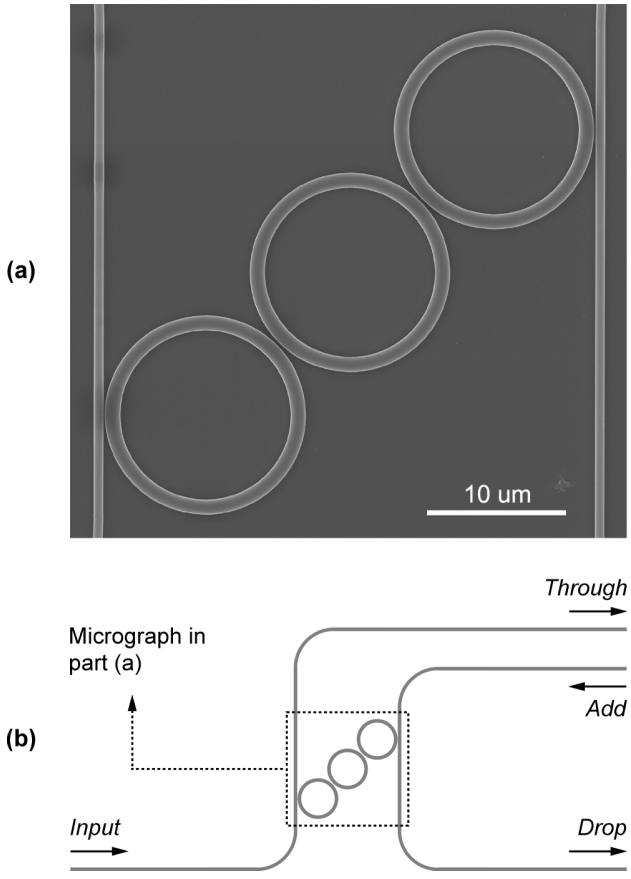

Fig. 2. Third-order add-drop filter based on series-coupled microring resonators. The rings' outer radius is 7.3 μm. The ring-to-bus gap is 60 nm and the ring-to-ring gap is 268 nm. (a) Scanning-electron micrograph. (b) Schematic of the chip layout used in the experiment. To ensure a reliable drop-loss measurement, the drop and the through waveguides traverse equivalent paths.

#4002 - $15.00 US Received 9 March 2004; revised 26 March 2004; accepted 29 March 2004

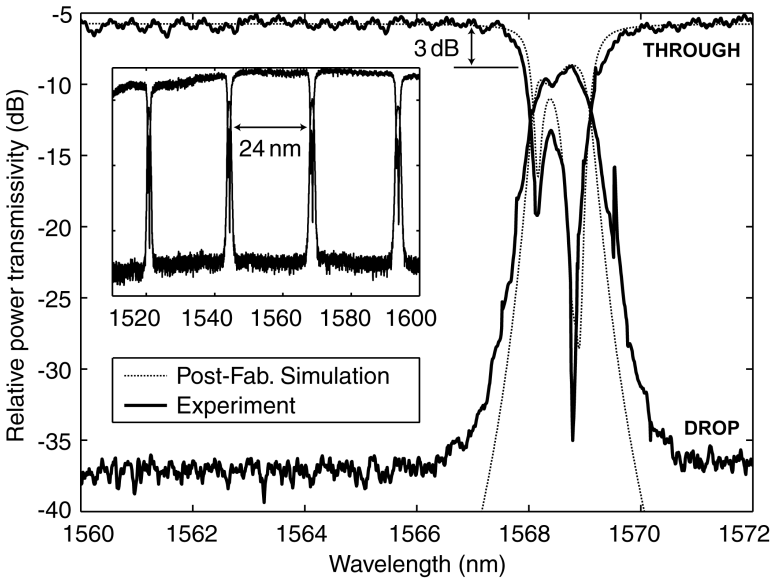

Fig. 3. Measured and simulated response of the third-order microring filter. The spectral asymmetry is due to frequency mismatch of resonators and can be compensated. Input-to-drop loss is dominated by scattering at the 60-nm-wide ring-bus coupler gaps. The narrow peak on the right of the drop spectrum is a measurement artifact. The inset shows several resonances and the free-spectral-range.

5. Discussion

Post-fabrication simulations were performed to understand the observed response of the fabricated third-order filter using the measured dimensions and refractive indices. Ring-ring and ring-bus coupling coefficients were calculated using three-dimensional finite-difference time-domain (FDTD) simulations. A cylindrical mode solver yielded bend losses and ring effective and group indices. The ring resonant frequencies were chosen to fit the data. These parameters, inserted into a transfer-matrix model for the filter, show agreement between theory and experiment (Fig. 3). The remaining difference may be explained by dimensional measurement errors.

The FDTD simulations indicate that additional losses were present in each of the rings due primarily to coupling to a lossy higher-order transverse mode of the ring waveguide at the couplers. The waveguides support a single mode of each polarization when straight, but when bent regain the second-order TE mode as a leaky resonance with high bend loss. This occurs because bending increases lateral confinement on the inner edge of the mode in addition to forcing leaky behavior beyond the radiation caustic. A higher-order mode can be tolerated if its loss is engineered to be high enough to ensure that it is not resonant and that no coupling to it from the fundamental mode is present. In our design, the 7 dB/90º of bending loss predicted for the second-order TE mode was sufficient to suppress its resonance, but turned out to be too low to forbid its excitation at the couplers by the fundamental resonance. This excitation translates to coupler losses, which are higher in the outer rings since the ring-bus coupling is stronger than the ring-ring coupling. The realized dimensions and indices give an expected radiation Q, due to bend loss, of 22 000. The coupler losses reduce the radiation Q's to about 10 000 (outer rings) and 13 000 (central ring). This reveals coupler scattering to be a significant loss mechanism. It and bend loss fully account for the observed drop loss (Fig. 3).

The spectral asymmetry, clear in the through-port response, is indicative of unequal, symmetrically distributed resonance frequencies, with the central ring having a higher frequency than the outer rings by 22 GHz. The effect is partially explained by coupling-

#4002 - $15.00 US Received 9 March 2004; revised 26 March 2004; accepted 29 March 2004

induced frequency shifting (CIFS) of resonators [8] due to the index perturbations caused by adjacent ring and bus waveguides. The CIFS calculated by FDTD is 43 GHz. Frequency shifts are also expected to result from dimensional variations in the rings due to e-beam proximity effects and e-beam discretization errors. While dimensional measurement uncertainty prevents a proper estimate of these effects, simple calculations reveal these effects to be of the same order as the CIFS. Proximity effects should contribute a shift of the same sign as the CIFS. Thus, we believe e-beam discretization errors are significant in reconciling the calculated CIFS with the experimentally-observed frequency shift.

The frequency mismatch can be corrected by properly predistorting the device design [8]. In practice, a slight, deliberate increase of e-beam dose on the middle ring could be applied. This would make the middle ring slightly wider and lower its resonant frequency to match it to the outer rings. The deleterious impact of uncompensated frequency mismatch will be less pronounced in filter designs that are intrinsically less sensitive to resonance frequency variations, such as those based on parallel-cascaded resonators [9-10]. These filters would also exhibit frequency shifts but their response would be less affected by them. In addition, their geometry may give these designs a smaller net frequency mismatch to begin with.

Despite the accurate fabrication of our filters, the measured 88 GHz bandwidth was more than twice the intended 40 GHz bandwidth. The matching of simulation results and experimental data supports the validity of the numerical simulations, and the discrepancy is attributed to the simple CMT design model. A larger-than-intended passband ripple limited in-band (through-port) rejection to 9 dB instead of an intended 13 dB. The resonant frequency mismatch further reduced this to 7.5 dB. These factors can be compensated to produce symmetric responses with stronger in-band rejection.

6. Conclusion

SiN microring-resonator-based add-drop filters were fabricated and characterized. Low filter loss and a large FSR were obtained without employing the Vernier effect. The filter response was measured and compared with rigorous post-fabrication simulations. Scattering at the ring-to-bus gaps and resonant frequency mismatch between the rings were found to degrade the filter response and to be correctable. A fabrication process yielding high resolution, accurate dimensional control and smooth waveguides was demonstrated. SiN has been shown to be a well-suited material for microring resonators.

Acknowledgments

We thank Christina Manolatou for use of her FDTD code, and J. Todd Hastings for help troubleshooting the Raith 150. This work was supported in part by Pirelli (Milan, Italy).

#4002 - $15.00 US Received 9 March 2004; revised 26 March 2004; accepted 29 March 2004